Measuring local CD uniformity in EUV vias with scatterometry and machine learning

Kong, Dexin, Schmidt, Daniel, Church, Jennifer, Liu, Chi-Chun, Breton, Mary, et al.

SPIE.

Measuring Local CD Uniformity in EUV vias with scatterometry and machine learning

Dexin Kong*[a], Daniel Schmidt[a], Jennifer Church[a], Chi-Chun Liu[a], Mary Breton[a], Cody Murray[a], Eric Miller[a], Luciana Meli[a], John Sporre[a], Nelson Felix[a], Ishtiaq Ahsan[a], Aron J. Cepler[b], Marjorie Cheng[b], Roy Koret[c], Igor Turovets[c]

[a]IBM, 257 Fuller Road, Albany, NY, 12203; [b]Nova Measuring Instruments, Inc., 3342 Gateway Blvd, Fremont CA 94538, USA; [c]Nova Measuring Instruments, LTD, 5 David Fikes St., P.O. Box 266, Rehovot 7610201, Israel

ABSTRACT

A methodology of obtaining the local critical dimension uniformity of contact hole arrays by using optical scatterometry in conjunction with machine learning algorithms is presented and discussed. Staggered contact hole arrays at 44 nm pitch were created by EUV lithography using three different positive-tone chemically amplified resists. To introduce local critical dimension uniformity variations different exposure conditions for dose and focus were used. Optical scatterometry spectra were acquired post development as well as post etch into a SiN layer. Reference data for the machine learning algorithm were collected by critical dimension scanning electron microscopy (CDSEM). The machine learning algorithm was then trained using the optical spectra and the corresponding calculated LCDU values from CDSEM image analyses. It was found that LCDU and CD can be accurately measured with the proposed methodology both post lithography and post etch. Additionally, since the collection of optical spectra post development is non-destructive, same area measurements are possible to single out etch improvements. This optical metrology technique can be readily implemented inline and significantly improves the throughput compared to currently used electron beam measurements.

Keywords: Scatterometry, machine learning, CDSEM, hybrid metrology, EUV, LCDU

1. INTRODUCTION

The local critical dimension uniformity (LCDU) as a result of an EUV lithography exposure must be monitored closely as it can have significant effects on defectivity and thus yield, particularly close to the resolution limit [1-5]. The LCDU is defined as the hole-to-hole (pillar-to-pillar) CD variation and is three times the standard deviation of the feature's average diameter [4]. It is a result of stochastic processes and sources include illumination conditions such as photon shot noise, dose, and focus as well as the characteristics of the involved materials such as the photoresists. It is important to measure the LCDU during the chip fabrication process in order to identify when it may be varying too far from the required device tolerances. Currently, most measurements of this metric are done with a critical dimension scanning electron microscope (CDSEM). The via structures as imaged by high-resolution CDSEM are measured invididually and subsequently the LCDU is calculated. However, this procedure comes with multiple drawbacks including small sample sizes at high magnifications, which are necessary to accurately image and measure individual vias as well as sample damage due to photoresist shrinkage post development [6].

This work explores the use of optical scatterometry in conjunction with machine learning in order to measure LCDU with higher throughput and without photoresist shrinkage. Optical scatterometry is an inline metrology technique, which is most commonly used to measure critical dimensions averaged over the probed area. However, by combining the measured spectra with machine learning, this technique can be used to measure average CD as well as the CD devation in the form of LCDU. Due to the intrinsic relationship between CD and LCDU [3], carefully designed experiments have been carried out to decouple both parameters and demonstrate that the proposed scatterometry-based technique can faithfully measure LCDU within a tight CD regime realistically found in a production environment.

2. EXPERIMENTAL DESIGN

A design-of-experiment (DOE) is set up in order to induce different amounts of LCDU. This variation in LCDU originates from the use of three different positive-tone chemically amplified photoresist materials as well as different dose and focus conditions during the exposure.
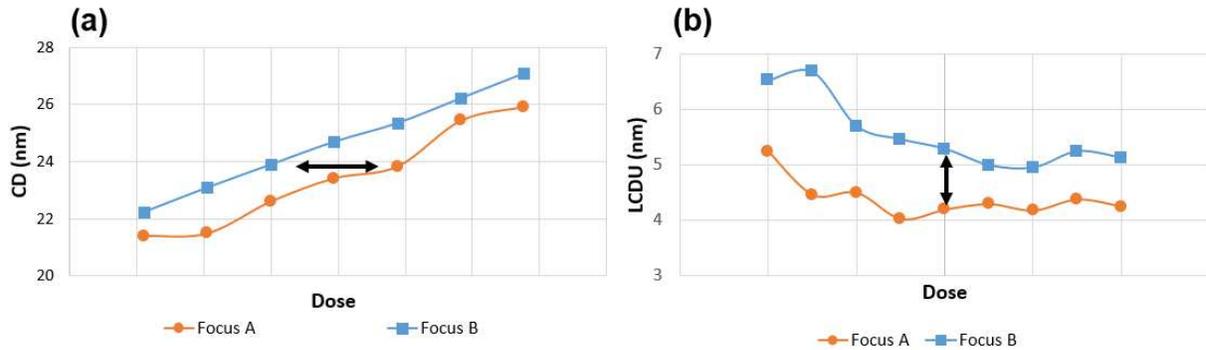

Figure 1: Representative CD (a) and LCDU (b) changes as a function of dose for two different focus conditions.

Figure 1 summarizes the relationships between lithographic parameters exposure dose and focus and the resulting CD and LCDU. Figure 1(a) shows that in oder to achieve a constant CD at different focus conditions a change in dose is required, while Figure 1(b) highlights that LCDU significantly changes for the two focus conditions, Focus A and Focus B. Therefore, dose and focus are the two knobs used for changing CD and LCDU and it is possible to find appropriate conditions leading to a variation in LCDU independent of CD.

Two DOEs are studied for this work: DOE1 uses a lithography material stack on bare silicon and DOE2 uses the lithography material stack on SiN-coated silicon. The DOE details are listed in Table 1 and Table 2. All wafers were exposed with dose stripes centered around the best dose for each photoresist, i.e. for each exposed die column the dose is increased stepwise from left to right across the wafer with the center column being exposed at best dose conditions. Note that larger dose steps were used for DOE1 as compared to DOE2. With its simple material stack DOE1 serves mainly feasability and evaluation purposes of the technique. The SiN layer used for DOE2 adds complexity and helps to demonstrate that the methodology can work independently of underlayers. Additionally, the presence of the underlayer allows the wafers to be further processed and then measure the LCDU again after the vias are etched into SiN.

Table 1: DOE1 conditions using a lithography material stack on a bare Si wafer; metrology is carried out post resist development only.

Exposure	Resist	Focus
1		+
2	Resist 1	Nominal
3		-
4		+
5	Resist 2	Nominal
6		-
7		+
8	Resist 3	Nominal
9		-

Table 2: DOE2 conditions using a lithography material stack on a SiN coated wafer; metrology is carried out post resist development and post etch into the SiN layer.

Exposure	Resist	Focus
1		+
2	Resist 1	Nominal
3		-
4		+
5	Resist 2	Nominal
6		-

3. EXPERIMENTAL METHODS

3.1 CDSEM

CDSEM is typically used in the semiconductor manufacturing process to measure lateral dimensions on the wafer [6]. To quantify LCDU, an image of a via array is captured by CDSEM, then the diameter is determined for each via individually and the standard deviation calculated. Depending on the amount of vias within one image, several images may need to be acquired for each die in order to get statistically significant LCDU values. One drawback of using CDSEM for measurements on photoresist is the risk of sample damage, as the interaction of the electron beam with the photoresist causes shrinkage, therefore permanently changing the dimension of the vias [6]. There can also be difficulties which arise as the algorithm separates between small changes in pixel gray levels to determine the location of an edge, which results in noise added to the data. The CDSEM images are acquired with a Hitachi CG5000 and an example is shown in Figure 2.
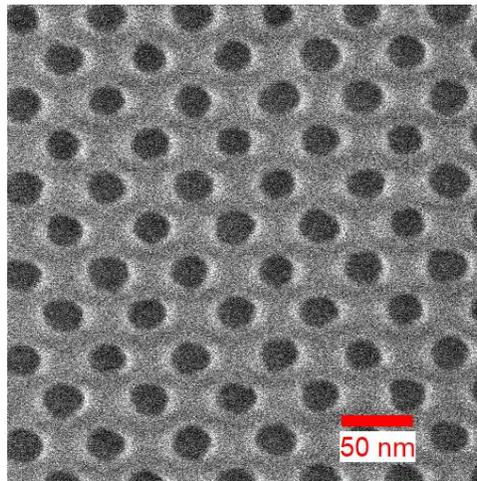

Figure 2: Example of a CDSEM image showing an array of staggered vias in resist after development.

3.2 Scatterometry and Machine Learning

Scatterometry is a metrology technique that is commonly used for fast and non-destructive measurements of dimensional and material parameters. **Error! Reference source not found.** shows a schematic explaining the operation of a scatterometry tool. A broad-band light source is illuminated to a spot on the wafer and the reflected light is collected across the wavelength range. Typically, a model is built based on the dimensional and optical

properties of the measured structure. An analytical method such as rigorous coupled-wave analysis (RCWA) is used to calculate the diffraction from the periodic array of structures and then interpret the measured spectra in a way such that dimensional and material information may be obtained [7-9]. As the technique requires diffraction from a periodic array, the tool measures an average quantity instead of a measurement from a single feature, in contrast to CDSEM, which can obtain measurements of discrete structures.
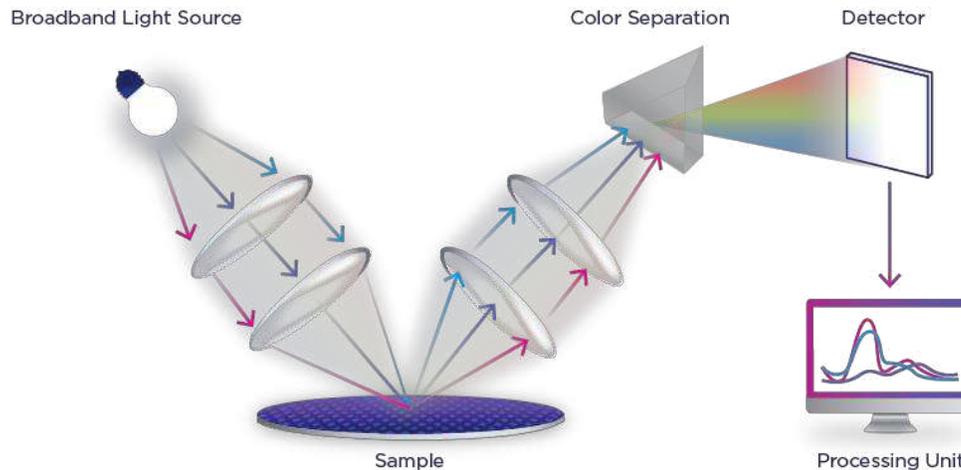

Figure 3: Schematic of optical scatterometry measurements.

In addition to traditional scatterometry modeling, machine learning can be used to directly link an external reference parameter with the measured spectra without the need for an optical model [10-16]. In this study, the measured values from the CDSEM image analysis are used as training parameters for a machine learning model and hence directly associated with acquired scatterometry spectra. Once the CDSEM data is made available for the initial training set, the machine learning model is trained to predict the LCDU. The scatterometry spectra are acquired with Nova T600MMSR, and the machine learning is done using Nova BrightFit.

4. RESULTS AND ANALYSIS

4.1 CDSEM sampling and filtering

When using CDSEM results to create a machine learning model for optical spectra acquired by scatterometry, it is important to understand certain differences between the tool sets that may affect the results. The CDSEM data is from a very small area with a field of view of typically only a few hundred nanometers, whereas the scatterometry spectra are acquired from a much larger spot with a diameter of about 25 μm. In this work, approximately 40 vias from an area less than 0.4×0.4 μm^2 are measured in a single CDSEM image; however, an average measurement result from scatterometry includes over 400,000 vias. In order to evaluate the via count mismatch and its effects on the quality of the machine learning training, multiple CDSEM images were acquired for each die and results from different counts of measured vias ranging from 32 to a maximum of 400 used for training. As shown in Figure 4, if only 32 vias are included, the match between the data from the machine learning model and the original CDSEM has a normalized correlation score of only 0.4. As the number of measured vias increases the correlation improves rapidly up to about 150 vias and then slower but continuously for increasing numbers. Therefore, nominally 180 and 400 vias for DOE1 and DOE2, respectively have been analyzed to calculate LCDU and average CD values used as reference data for the machine learning model training.

An additional aspect that must be addressed for successful machine learning training based on limited sampling is to eliminate possible outliers in the reference data set. This is particularly important in the current study, because the large dose and focus regimes selected within the DOE span beyond the process window in each parameter dimension. Hence, the increased defect densities at the extremes may create problems for automatic CDSEM image-analysis algorithms.
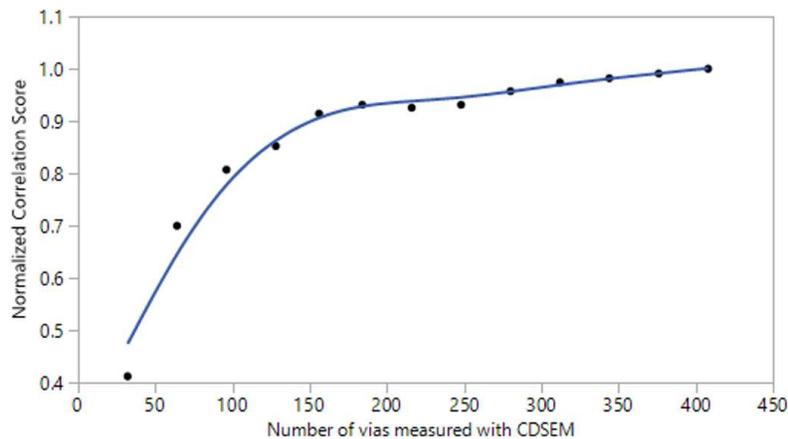
Figure 4: Normalized correlation between CDSEM and Machine Learning results as a function of measured vias. The machine learning model results improve significantly when increasing the number of measured vias. The solid line serves as a guide to the eye.

Analysis of CDSEM images and via shapes showed that the main problems are related to the treatment of merged vias and irregular contours occuring mainly at doses above the nominal value. The effect of CDSEM data filtering of outliers was evaluated for both CD (via diameter) and LCDU values. A representative comparison between the original and the filtered data set of the average via diameter is shown in Figure 5. This filter aims at removing individual diameter outliers that are either caused by pattern defects (missing or merged vias) or image analysis defects. The application of this filter has negligible impact on the average via diameter for any of the three depicted focus conditions, as shown in Figure 5(a). The relative number of removed data points by the algorithm is plotted as function of location on the wafer in Figure 5(b). While a small fraction of data points are removed across the wafer, the number increases towards the right side of the wafer, which corresponds to high dose exposures and consequently an increased occurance of merged via defects.
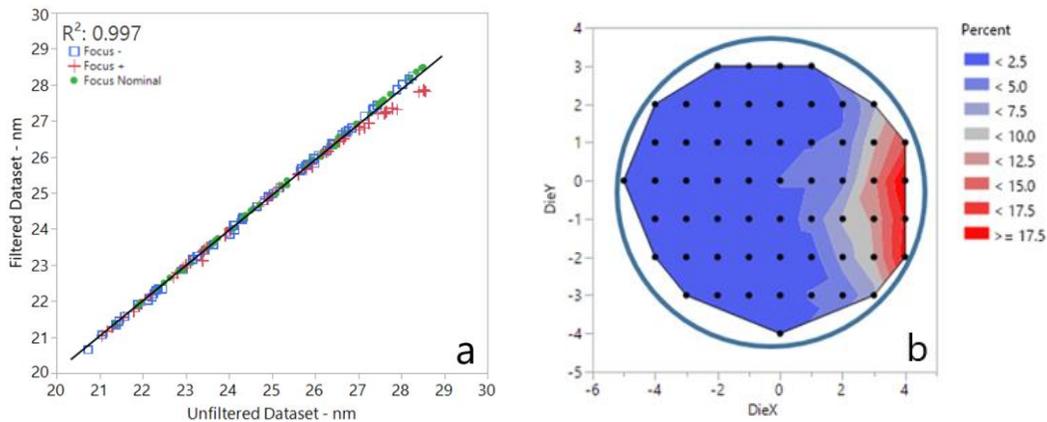

Figure 5: Effects of filtering on the CDSEM dataset. (a) Comparison between the average diameter results of the filtered and the unfiltered CDSEM data set for Resist 2 of DOE1. (b) Example wafer map showing the relative amount of removed vias by the applied filter of Exposure 4 (DOE1). Most outliers are found on the right side of the wafer, corresponding with higher doses.

Figure 6 shows the CDSEM LCDU data post etch (Exposure 4, DOE2) as an example of before and after final data filtering, which includes outlier removal as discussed above and an additional data treatment aimed at mitigating the differences related to the number of vias measured with each tool. It can be stated that on average the applied filtering does not have a significant effect on the final uniformity result but rather removes outliers and results in a slightly

smoother transition from the left side (low dose condition) toward the right side of the wafer (high dose condition). Such a smooth transition with a minimum in the center is expected here as the center column of the wafer is exposed at best dose conditions and LCDU is expected to increase when moving away from the nominal conditions. Using the filtered LCDU data set as a reference improved the machine learning significantly.
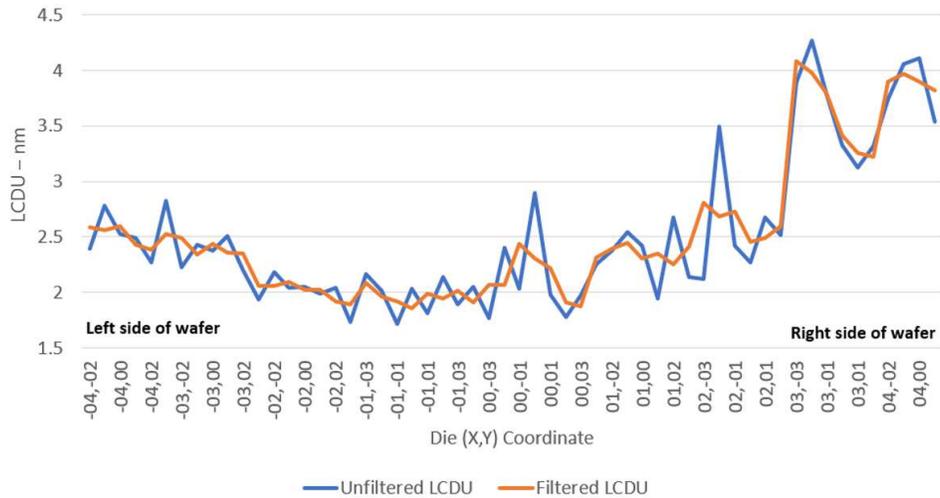

Figure 6: CDSEM LCDU results before and after final filtering as a function of die coordinate sorted by locations on the wafer from left to right. A single dose stripe wafer post etch is shown as a representative example (DOE2, Exposure 4) and a total of 56 measurements locations across the wafer. The increase of LCDU at the left and right side is due to dose conditions below and above nominal, respectively.

4.2 Machine Learning for Via CD

In order to set a machine learning benchmark for direct association of CDSEM measurements with scatterometry spectra, the via diameter is examined as a test case. Results for Resist 1 with exposures from DOE1 as an example are shown in Figure 7. As designed by experimental conditions, all three focus conditions lead to an approximatley equal diameter range as a result of the dose stripe exposures. A very good correlation ($R^2 > 0.97$) between the output from the machine learning model and the CDSEM reference data for all studied resists and exposure conditions is achieved.
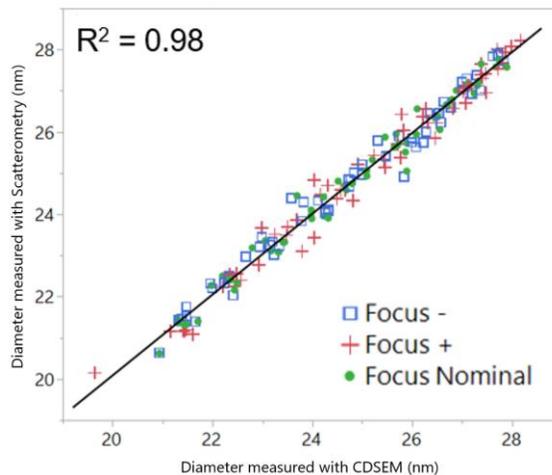

Figure 7: Comparison of via diameter of Resist 1 as measured by CDSEM and scatterometry for all three focus conditions (DOE1 only).

4.3 Scatterometry measurement of LCDU

First, the results for scatterometry with machine learning to measure LCDU on wafers with the lithography stack on bare silicon wafers are presented, based on the DOE1 shown in Table 1. Three different photoresists are exposed with varying focus conditions from wafer to wafer, and the dose is varied within each wafer. Figure 8 shows the LCDU from scatterometry with machine learning as compared to LCDU from CDSEM. Excellent correlations are seen for all three photoresist and Resists 1 and 3 exhibit R^2 values greater than 0.9. The lower R^2 for Resist 2 can be attributed mainly to the smaller range in LCDU compared to the other two resists since the out-of-focus and nominal exposure conditions here are yielding similar LCDU values.
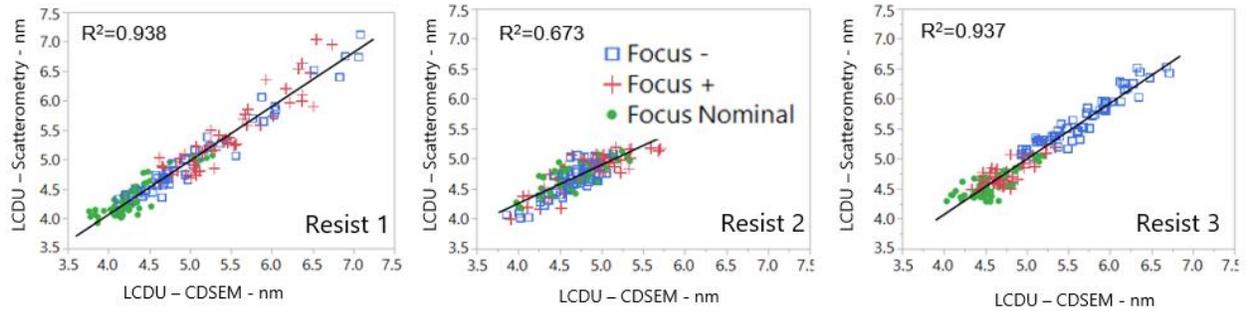

Figure 8: LCDU from CDSEM compared to LCDU from scatterometry for DOE1. For each of the three resists all three focus conditions are plotted.

In Figure 9, LCDU results obtained from both techniques are plotted separately versus dose for each of the three resists. This figure highlights that the dose and focus dependence of LCDU measured from scatterometry matches very well with that from CDSEM. At each dose condition, several dies within the iso-dose column are measured and the distribution of results from scatterometry is on average slightly smaller than from CDSEM. This is attributed to the measurement area sizes between the two techniques leading to LCDU results from via counts, which differ by approximately three orders of magnitude. Consequently, LCDU results obtained from scatterometry are statistically more representative of the overall process capabilities.
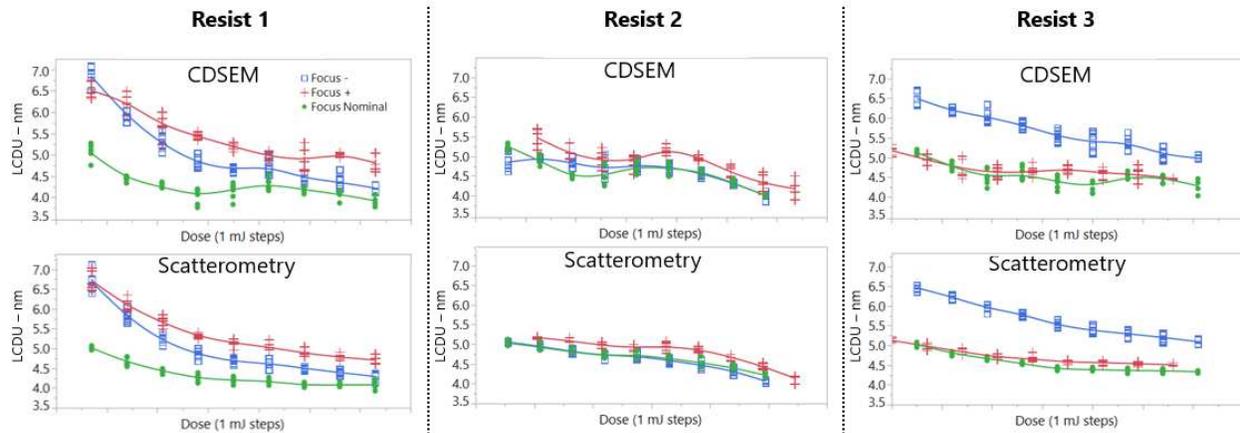

Figure 9: LCDU as a function of dose for CDSEM and Scatterometry. Dose values on the *x* axis are centered around the best dose condition for each resist.

Next, the experiment is repeated for Resists 1 and 2 using a lithography material stack on top of SiN coated wafers instead of bare Si wafers (see Table 2). The purpose of this experiment is twofold: (1) demonstrate LCDU measurements on wafers with increased experimental complexity (added SiN layer including small thickness varations across the wafer), as well as (2) enabling measurements both post lithography and post etch. Figure 10 shows the

excellent results obtained with this method post lithography despite the more complex scenario. Hence, underlayers with associated non-idealities (e.g. thickness or density variations) do not impact the analysis and scatterometry in conjunction with machine learning is capabale of delivering LCDU results on relevant stacks as found in production environments.
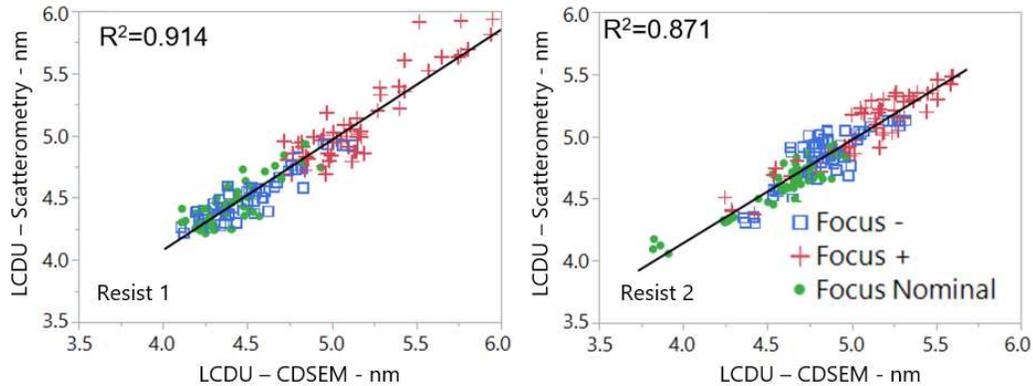

Figure 10: LCDU from CDSEM compared to LCDU from scatterometry for DOE2. For both resists all three focus conditions are plotted.

After measurements from the post-lithography step were completed, the DOE2 wafers were moved to the etch processing step and subsequently measured again. Due to photoresist damage as a result of electron beam exposure during CDSEM image acquisition discussed earlier, the CDSEM measurements post development and post etch cannot originate from the same area. Hence, in order to probe LCDU post development and post etch the CDSEM metrology areas must be offset, which may not necessarily result in an accurate comparison, depending on the total via count, as site-to-site differences can negatively influence the readings. In contrast, scatterometry does not cause photoresist shrinkage and the measurement locations can be identical at both processing steps. Figure 11 depicts the very good agreement between the LCDU measured with CDSEM and scatterometry at both process steps and for both resists ($R^2 = 0.98$). It is also observed that as the wafers undergo etch the LCDU is significantly reduced, and that Resist 1 produces better LCDU than Resist 2 even though both resists exhibit a similar LCDU post development.
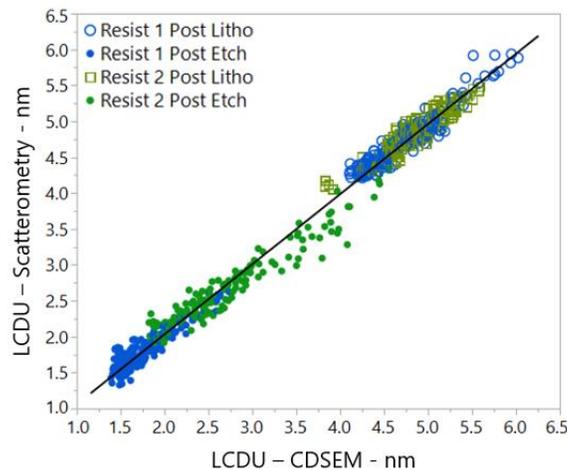

Figure 11: LCDU from CDSEM compared to LCDU from scatterometry for DOE2 post litho and post etch combined. An R^2 of 0.98 is achieved between the CDSEM and scatterometry results.

All results shown so far are using wafers exposed with dose stripe conditions thereby inducing a large range of LCDU values. However, wafers in a high volume manufacturing environment are exposed at nominal conditions only and

any dose or focus distribution is due to noise and other non-idealities. In order to evaluate if LCDU measurements with scatterometry are valid for a production-type environment, a limited dataset is selected, which is restricted to dies with vias that have diameters within a 1 nm range. Furthermore, the selection of this data set with tight CD distribution would reveal any correlation between LCDU and CD. Figure 12 shows that also in this case a good agreement between CDSEM and scatterometry with $R^2 > 0.7$ is achieve. These results demonstrate that the scatterometry-based method truly measures the LCDU and is a suitable technique for monitoring in high volume manufacturing.
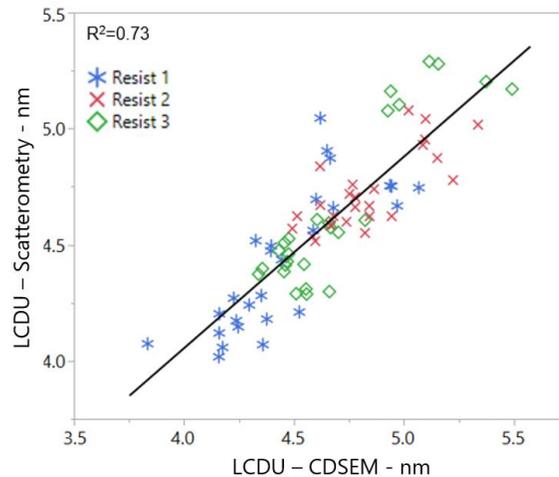

Figure 12: LCDU from CDSEM compared to LCDU from scatterometry for vias with near-nominal CD only (1 nm range) selected from available data points from DOE1.

5. CONCLUSIONS

A new methodology to measure LCDU using optical scatterometry with machine learning was developed and discussed. The reference data used to train the machine learning algorithm were obtained by analyzing CDSEM images with subsequent filtering to remove outliers and mitigating the differences related to the number of vias measured with each tool. This presented machine learning technique was found to be valid post development and post etch. Excellent correlation with reference metrology was achieved for all three photoresists under investigation and on more complex stacks highlighting that this methodology is suitable for in-line characterization. This production monitoring readiness is further supported by the metrology demonstration of small LCDU variations after development. Since the collection of optical spectra post development is non-desctructive, measurements within the same area post etch are possible thereby providing valuable information about litho and etch conditions individually enabling uncorrelated process improvement for efficient overall best LCDU results.

This presented novel method has significant advantages over the current CDSEM-based approach with regards to throughput (for example, one scatterometry measurement may replace multiple CDSEM measurements per site) and sample damage (photoresist shrinkage from the electron beam). The fact that the scatterometry beam probes an area approximately three orders of magnitude larger compared to CDSEM has to be considered when 'local' uniformity is desired. However, since scatterometry yields LCDU from a much larger via count the results are statisctically more accurate and less prone to localized non-idealities and defects.

ACKNOWLEDGEMENTS

REFERENCES

1. Chris Mack, "Stochastic limitations to EUV lithography", 2018 International Symposium on VLSI Technlogy, Systems and Application (2018).

2. Timothy Brunner, Xuemei Chen, et al., "Line-Edge Roughness performance targets for EUV Lithography", Proc. SPIE 10143, Extreme Ultraviolet (EUV) Lithography VIII, 10143 (2017).

3. Chris Mack, "Metrics for stochastic scaling in EUV Lithography", Proc. SPIE 11147, International Conference on Extreme Ultraviolet Lithography 2019, 11147 (2019).

4. Andrew Liang, et al., "Integrated approach to improving local CD uniformity in EUV patterning", Proc. SPIE 10143, Extreme Ultraviolet (EUV) Lithography VIII, 1014319 (2017).

5. Zhengqing John Qi, Jed Rankin, Lei Sun, and Harry Levinson, "Contribution of EUV mask CD variability on LCDU", Proc. SPIE 10143, Extreme Ultraviolet (EUV) Lithography VIII, 101431Y (2017).

6. Shimon Levi, "EUV photo resist shrink characterization using low landing energy SEM (Conference Presentation)", Proc. SPIE 11325, Metrology, Inspection, and Process Control for Microlithography XXXIV, 113251S (2020).

7. Christopher Raymond, "Overview of Scatterometry Applications in High Volume Silicon Manufacturing", Characterization and Metrology for ULSI Technology, CP 788, 2005.

8. Shacham-Diamand, Y., Osaka, T., Datta, M., and Ohba, T. Advanced Nanoscale ULSI Interconnects: Fundamentals and Applications. Springer, NY,481-484, 2009.

9. Dror Shafir, Gilad Barak, et. al., "Mueller matrix characterization using spectral reflectometry." Proc. SPIE 8789, Modeling Aspects in Optical Metrology IV, 878903 (2013).

10. D. Kong, RHK Chao, H Huang, "Measuring Defectivity by Equipping Model-Less Scatterometry with Cognitive Machine Learning", US Patent App. 15/899,197, 2019.

11. RHK Chao, M Breton, H Huang, D Kong, LA Clevenger, "Machine learning enhanced optical-based screening for in-line wafer testing", US Patent App. 16/110,048, 2020.

12. Narender Rana, Yunlin Zhang, et. al., "Leveraging advanced data analytics, machine learning, and metrology models to enable critical dimension metrology solutions for advanced integrated circuit nodes", J. of Micro/Nanolithography, MEMS, and MOEMS, 13(4), 041415 (2014).

13. Mary Breton, Robin Chao, et al., "Electrical test prediction using hybrid metrology and machine learning", Proc. SPIE 10145, Metrology, Inspection, and Process Control for Microlithography XXXI, 1014504 (2017).

14. Dexin Kong, Robin Chao, et al., "In-line characterization of non-selective SiGe nodule defects with scatterometry enabled by machine learning", Proc. SPIE 10585, Metrology, Inspection, and Process Control for Microlithography XXXII, 1058510 (2018).

15. Dexin Kong, Koichi Motoyama, et al., "Machine learning and hybrid metrology using scatterometry and LE-XRF to detect voids in copper lines", Proc. SPIE 10959, Metrology, Inspection, and Process Control for Microlithography XXXIII, 109590A (2019).

16. Sayantan Das, Joey Hung, et. al., "Machine learning for predictive electrical performance using OCD", Proc. SPIE 10959, Metrology, Inspection, and Process Control for Microlithography XXXIII, 109590F (2019).